
The Graph Hawkes Network for Reasoning on Temporal Knowledge Graphs

Zhen Han

LMU Munich & Siemens AG
Otto-Hahn-Ring 6
81739 Munich
han.zhen@siemens.com

Yuyi Wang

ETH Zürich
Rämistrasse 101
8092 Zürich
yuwang@ethz.ch

Yunpu Ma*

LMU Munich & Siemens AG
Otto-Hahn-Ring 6
81739 Munich
cognitive.yunpu@gmail.com

Stephan Günnemann*

Technical University of Munich
Boltzmannstr. 3
85748 Garching b. München
guennemann@in.tum.de

Volker Tresp*

LMU Munich & Siemens AG
Otto-Hahn-Ring 6
81739 Munich
volker.tresp@siemens.com

Abstract

The Hawkes process has become a standard method for modeling self-exciting event sequences with different event types. A recent work generalizing the Hawkes process to a neurally self-modulating multivariate point process enables the capturing of more complex and realistic influences of past events on the future. However, this approach is limited by the number of event types, making it impossible to model the dynamics of evolving graph sequences, where each possible link between two nodes can be considered as an event type. The problem becomes even more dramatic when links are directional and labeled, since, in this case, the number of event types scales with the number of nodes and link types. To address this issue, we propose the Graph Hawkes Network to capture the dynamics of evolving graph sequences. Extensive experiments on large-scale temporal relational databases, such as temporal knowledge graphs, demonstrate the effectiveness of our approach.

1 Introduction

If the value of the dollar weakens against other major currencies, will the price of the oil go up? And especially when will it go up? Modeling the relevant events that can affect or be affected by the dollar's value as well as the oil prices is the key to answer this question. However, how to model these complicated temporal events is an intriguing question. A possible way is to embed these events in a temporal knowledge graph, which is a graph-structured relational database that stores an event in the form of a quadruple. Besides, point processes are powerful mathematical tools for modeling temporal events and have been widely applied to many real-world applications such as the analysis of social networks (Zhou et al., 2013), the prediction of recurrent user behaviors (Du et al., 2016), and the estimation of consumer behaviors in finance (Bacry et al., 2016). The well known **Poisson**

process (Palm, 1943) is limited to modeling temporal events that occur independently of one another. To model correlated event sequences, Hawkes (1971) proposed a self-exciting point process, which is now known as the **Hawkes process**. The Hawkes process assumes that past events have an excitation effect on the likelihood of future events, and such excitation exponentially decays with time. This model is useful in some domains such as modeling earthquakes (Ogata, 1998). However, it is unable to capture some real-world patterns where past events of a different type may have inhibitory effects on future events, i.e., a skateboard purchase may inhibit a bike purchase. To address this limitation, the neural Hawkes process (Mei & Eisner, 2017) generalized the Hawkes process using recurrent neural networks with continuous state spaces such that past events can excite and inhibit future events in a complex and realistic way. Nevertheless, the neural Hawkes process is only capable of modeling event sequences with a small number of event types and fails to accurately capture the mutual influence in large-scale temporal relational data. An example would be the evolving links in a dynamic graph sequence where the connections between nodes can be considered as different event types. The problem becomes even more challenging when the links are directional and labeled. In order to model the dynamics of directional and labeled links in a graph sequence, we develop a novel Graph Hawkes Process and apply it to large-scale temporal relational databases, such as temporal knowledge graphs.

Before introducing temporal knowledge graphs, we briefly review semantic knowledge graphs (semantic KGs), which are relational knowledge bases for storing factual information. Semantic KGs such as the Google Knowledge Graph (Singhal, 2012) and NELL (Carlson et al., 2010) represent an event as a semantic triple (s, p, o) in which s (subject) and o (object) are entities (nodes), and p (predicate) is a directional labeled link (edge). Latent feature models (Ma et al., 2018; Nickel et al., 2011) and graph feature models (Minervini et al., 2014; Liu & Lü, 2010) are two popular approaches to develop statistical models for semantic KGs. However, in contrast to static relational data in semantic KGs, entities and their relations in many real-world scenarios are not fixed and may change over time. Such temporal events can be represented as a quadruple (s, p, o, t) by extending the semantic triple with a timestamp t describing when these events occurred. Further an event may last for a period of time. For example, (John, lives in, Vancouver) could be true for many time steps, and (Alice, knows, John) might be true always. We can simply discretize such an event into a sequence of time-stamped events to store it in the form of quadruples. Figure 1 shows an example of a temporal KG. By considering time, the semantic KGs are augmented into **temporal knowledge graphs** (tKGs), which creates the need for statistical learning that can capture dynamic relations between entities in tKGs. Modeling dynamic relations between entities over tKGs becomes more challenging than normal event streams since the number of event types is of order $N_e^2 \cdot N_p$, where N_e and N_p are the number of entities and predicates respectively. Recent studies on tKGs reasoning focussed on augmenting entity embeddings with time-dependent components in a low-dimensional space (Kazemi, Goel, Eghbali, et al., 2019; Sankar et al., 2018). However, these models either lack a principled way to predict the occurrence time of future events (Jin et al., 2019; Leblay & Chekol, 2018; García-Durán et al., 2018) or ignore the concurrent entity interactions within the same time slice (Trivedi et al., 2017).

In this paper, we propose a novel deep learning architecture to capture temporal dependencies on tKGs, called **Graph Hawkes Network** (GHN). More specifically, our main contributions are:

- We propose a Graph Hawkes Network for reasoning over large-scale tKGs. This is the first work that uses the Hawkes process to interpret and capture the underlying temporal dynamics of entity interactions in tKGs.
- Different from the previous tKG models with discrete state spaces, we model a discrete event in tKGs in continuous time. In this way, our model can compute the probability of an event at an arbitrary timestamp, which considerably enhances model flexibility..
- We analyze previous problematic evaluation metrics and propose a new ranking metric for link prediction on temporal knowledge graphs.
- Compared to current state-of-the-art time prediction models on tKGs, our approach can perform long-term predictions and achieve more accurate results.

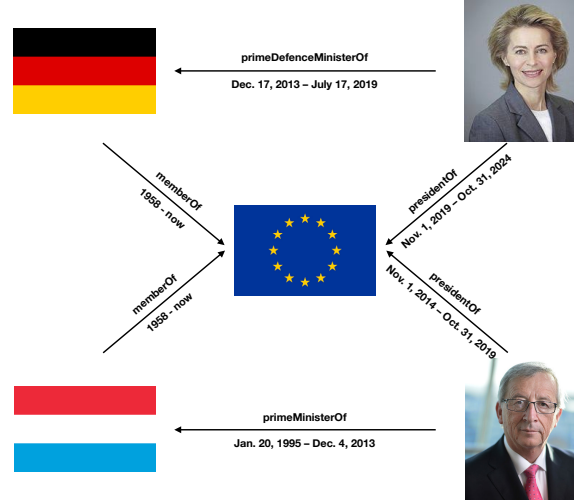


Figure 1: Illustration of a temporal knowledge graph between persons and countries.

2 Background and Related Work

2.1 The Hawkes Process

The Hawkes process is a stochastic process for modeling sequential asynchronous discrete events occurring in continuous time where asynchronous means that the time intervals between consecutive events may not be identical (Kazemi, Goel, Jain, et al., 2019). Moreover, the Hawkes process supposes that past events can temporarily excite future events, which is characterized via the intensity function defined as follows:

$$\lambda_k(t) = \mu_k + \sum_{t_{k_h} < t} \alpha_{k_h, k} \exp(-\delta_{k_h, k}(t - t_{k_h})) \quad (1)$$

where $\mu_k \geq 0$ is the time-independent base intensity of an event type k , $\alpha_{k_h, k} \geq 0$ is the degree to which an event of type k_h instantaneously excites type k , and $\delta_{k_h, k} > 0$ is the decay rate of that excitation (Mei & Eisner, 2017). The intensity function $\lambda_k(t)$ represents the expected number of events with type k in the interval of unit length. Thus, according to the survival analysis theory (Aalen et al., 2008), the density function that an event with the type k occurs at t_i is defined as the product of its intensity function at t_i and the probability that no event happens from t_L till t_i :

$$p_k(t_i) = \lambda_k(t_i) \exp\left(-\int_{t_L}^{t_i} \sum_k \lambda_k(s) ds\right) \quad (2)$$

where t_L denotes the latest happening time of an event without regarding its event type.

2.2 Temporal Knowledge Graph Reasoning

Temporal knowledge graphs are multi-relational, directed graphs with labeled timestamped edges (predicates) between nodes (entities) (Trivedi et al., 2017). Each timestamped edge represents a specific event that is formed by a predicate edge p between subject entity s and object entity o at timestamp t and is denoted by a quadruple (e_s, e_p, e_o, t) , where $e_s, e_o \in \{1, \dots, N_e\}$, $e_p \in \{1, \dots, N_p\}$, $t \in \mathbb{R}^+$. A tKG can therefore be represented as an ordered sequence of quadruples, $\mathbb{E} = \{e_i = (e_{s_i}, e_{p_i}, e_{o_i}, t_i)\}_{i=1}^N$, where $0 \leq t_1 \leq \dots \leq t_n$. One of the fundamental reasoning task in tKGs is to predict unseen links between entities. A classical task is to predict either a missing subject entity $(?, e_{p_i}, e_{o_i}, t_i)$ or a missing object entity $(e_{s_i}, e_{p_i}, ?, t_i)$. While one aims to predict the missing entities in the existing graphs in the context of a semantic knowledge graph, one may want to predict the missing entities in the future timestamp t_i based on observed events occurred before t_i . Besides predicting which event will happen in the future, another challenging problem is to predict

when an event will happen, which is referred as the time prediction task. More concretely, one can precisely answer questions like:

- **Object prediction.** Which country will Donald Trump visit next?
- **Subject prediction.** Who is the wife of Donald Trump?
- **Time prediction.** When will Donald Trump tweet again?

Recently, several studies focussed on temporal knowledge graph reasoning. Esteban et al. (2016) introduced an event model for modeling the temporal evolution of KGs where the prediction of future events is based on the latent representations of the knowledge graph tensor and of the time-specific representations from the observed event tensor. Jiang et al. (2016) augmented some existing static knowledge graph models (Bordes et al., 2013; Wang et al., 2014; Lin et al., 2015) with temporal consistency constraints such as temporal order information so that the time-aware inference can be formulated as an Integer Linear Program problem with temporal constraints. In addition, Ma et al. (2018) developed extensions of static knowledge graphs such as **Complex** (Trouillon et al., 2017) and **RESCAL** (Nickel et al., 2011) by adding a timestamp embedding to their score functions. Besides, Leblay & Chekol (2018) incorporated time presentations into score functions of several static KG models such as **TransE** (Bordes et al., 2013) and **RESCAL** (Nickel et al., 2011) in different ways. Additionally, García-Durán et al. (2018) suggested a straight forward extension of some existing static knowledge graph models (Bordes et al., 2013; Yang et al., 2014) that utilize a recurrent neural network (RNN) to encode predicates with temporal tokens derived by decomposing given timestamps. Also, **HyTE** (Dasgupta et al., 2018) embeds time information in the entity-relation space by arranging a temporal hyperplane to each timestamp. However, the aforementioned models (Ma et al., 2018; Trouillon et al., 2017; Nickel et al., 2011) cannot predict future events, they are only models for temporal KGs **COMPLETION**. In contrast, **AiTSEE** (Xu et al., 2019) directly incorporates time as a scale into entity representations by utilizing the linear time series decomposition. However, these models do not capture temporal dynamics and cannot generalize to unseen timestamps because their models only take the current time information into account (Jin et al., 2019). In contrast, **Know-Evolve** (Trivedi et al., 2017) learns evolving entity representations using the Rayleigh process, being able to capture the dynamic characteristics of tKGs. Additionally, **RE-Net** augmented the **R-GCN** model (Schlichtkrull et al., 2018) to the tKGs and uses the order of history event for predicting the future. Moreover, Trivedi et al. (2018) argued that different dynamics might evolve at different time-scales, e.g., the association process (liking posts in a social network) evolves more frequently than the communication process (liking forming a new friendship); thus, they proposed the **DyRep** parameterized by a temporal attention mechanism to capture dynamics with different evolving rate.

3 Notation

Throughout the following sections, e_i denotes an event consisting of $(e_{s_i}, e_{p_i}, e_{o_i})$ where e_{s_i} , e_{o_i} and e_{p_i} written not in bold represent the subject entity, object entity and predicate of the event e_i , respectively. Additionally, we use t_i denote the timestamp when the event e_i occurred. Besides, \mathbf{e}_{s_i} , \mathbf{e}_{p_i} , \mathbf{e}_{o_i} written in bold represent their embeddings.

We denote vectors by bold lowercase letters such as \mathbf{c} and \mathbf{h} , and matrices by bold capital Roman letters, e.g., \mathbf{W} . Additionally, subscripted bold letters denote specific vectors or matrices such as \mathbf{k}_m . Moreover, scalar quantities such as λ_k and $\delta_{k,j}$, are written without bold. We denote the upper limits of scalar quantities by capitalized scalars, for example, $1 \leq n \leq N$.

4 Our Model

In this section, we present the Graph Hawkes Network (GHN) for capturing mutual influence in large-scale multi-relational graph sequences that can be seen as an event stream with a large amount of event types. The GHN consists of the following two major modules:

- A Graph Hawkes Process for modeling the occurrence of a fact where we use a recurrent neural network to learn this temporal point process.
- A neighborhood aggregation module for capturing the information from concurrent events that happened at the same timestamp.

We take the temporal knowledge graph as an example and show how our model deals with the link prediction task and the time prediction task on temporal knowledge graphs. Besides, the GHN also learns latent representations specified for entities and predicates. In the rest of this section, we first define the relevant historical event sequence for each inference task, which is the input of the Graph Hawkes Network, and then provide details on the proposed modules in the Graph Hawkes Network.

4.1 Relevant Historical Event Sequences

By viewing a temporal knowledge graph \mathcal{G} as a sequence of graph slices $\{\mathcal{G}_1, \mathcal{G}_2, \dots, \mathcal{G}_T\}$ where $\mathcal{G}_t = \{(e_s, e_p, e_o, t') \in \mathcal{G} | t' = t\}$ denote a graph slice that consists of events that occurred at the timestamp t . Thus, we can model the joint probability of a temporal knowledge graph \mathcal{G} as:

$$\begin{aligned} \mathbb{P}(\mathcal{G}) &= \mathbb{P}(\mathcal{G}_1, \mathcal{G}_2, \dots, \mathcal{G}_T) \\ &= \prod_{t=1}^T \mathbb{P}(\mathcal{G}_t | \mathcal{G}_{t-1}, \mathcal{G}_{t-2}, \dots, \mathcal{G}_1) \end{aligned} \quad (3)$$

Inspired by (Jin et al., 2019), we assume that concurrent events belonging to the same graph slice, which means that they occurred at the same timestamp, are conditionally independent to each other given the observed graph slices. Thus, we can write the conditional probability of a graph slice \mathcal{G}_t as follows:

$$\mathbb{P}(\mathcal{G}_t | \mathcal{G}_{t-1}, \mathcal{G}_{t-2}, \dots, \mathcal{G}_1) = \prod_{e_i \in \mathcal{G}_t} \mathbb{P}(e_i | \mathcal{G}_{t-1}, \mathcal{G}_{t-2}, \dots, \mathcal{G}_1) \quad (4)$$

where e_i denotes an event belonging to \mathcal{G}_t . Thus, for predicting a missing object entity of a object prediction query $(e_{s_i}, e_{p_i}, ?, t_i)$, we can simply compare the conditional probability $\mathbb{P}(e_o | e_{s_i}, e_{p_i}, t_i, \mathcal{G}_{t_{i-1}}, \mathcal{G}_{t_{i-2}}, \dots, \mathcal{G}_1)$ of all object entity candidates. To further make large-scale temporal knowledge graphs tractable, we assume that the conditional probability that an object entity interacts with a given subject entity e_{s_i} with respect to a predicate e_{p_i} at a timestamp t_i mainly depends on past events that include e_{s_i} and e_{p_i} . We define these relevant events as the relevant historical event sequence $e_i^{h,sp}$ for predicting the missing object entity e_{o_i} :

$$e_i^{h,sp} = \left\{ \bigcup_{0 \leq t_j < t_i} (e_{s_i}, e_{p_i}, \mathbf{O}_{t_j}(e_{s_i}, e_{p_i}), t_j) \right\} \quad (5)$$

where $\mathbf{O}_{t_j}(e_{s_i}, e_{p_i})$ is a set of object entities that interacted with the subject entity e_{s_i} under the predicate e_{p_i} at a timestamp t_j ($0 \leq t_j < t_i$). Thus, we can rewrite the conditional probability of an object entity candidate e_o given a query $(e_{s_i}, e_{p_i}, ?, t_i)$ and past $i-1$ graph slices into the following form:

$$\begin{aligned} \mathbb{P}(e_o | e_{s_i}, e_{p_i}, t_i, \mathcal{G}_{t_{i-1}}, \mathcal{G}_{t_{i-2}}, \dots, \mathcal{G}_1) \\ = \mathbb{P}(e_o | e_{s_i}, e_{p_i}, t_i, e_i^{h,sp}). \end{aligned} \quad (6)$$

To capture the impact of other past events that have different subject entity or predicate than the query has, we use a shared latent representation for an entity appeared in different queries. For each observed event in the training set, two entities involved in the event propagate information from the neighborhood of one entity to the other entity. Thus, after training, the model is also able to capture dynamics between multi-hop neighbors with various relations.

Similarly, we define a relevant historical event sequence $e_i^{h,op}$ for predicting the missing subject entity e_{s_i} given a subject prediction query $(?, e_{p_i}, e_{o_i}, t_i)$:

$$e_i^{h,op} = \left\{ \bigcup_{0 \leq t_j < t_i} (e_{o_i}, e_{p_i}, \mathbf{S}_{t_j}(e_{o_i}, e_{p_i}), t_j) \right\} \quad (7)$$

where $\mathbf{S}_{t_j}(e_{o_i}, e_{p_i})$ is a set of subject entities that interacted with the object entity e_{o_i} under the predicate e_{p_i} at a timestamp t_j with the restriction of $0 \leq t_j < t_i$. Thus, we can rewrite the conditional probability of a subject entity candidate e_s given a query $(?, e_{p_i}, e_{o_i}, t_i)$ and past $i-1$ graph slices into the following form:

$$\begin{aligned} \mathbb{P}(e_s | e_{o_i}, e_{p_i}, t_i, \mathcal{G}_{t_{i-1}}, \mathcal{G}_{t_{i-2}}, \dots, \mathcal{G}_1) \\ = \mathbb{P}(e_s | e_{o_i}, e_{p_i}, t_i, e_i^{h,op}). \end{aligned} \quad (8)$$

For the time prediction task, we assume that the time of the next occurrence of a triplet $(e_{s_i}, e_{p_i}, e_{o_i})$ is mainly dependent on past events that include either (e_{s_i}, e_{p_i}) or (e_{o_i}, e_{p_i}) . This gives the conditional probability density function at a timestamp t given a query $(e_{s_i}, e_{p_i}, e_{o_i}, ?)$ and past $i - 1$ graph slices with the following form:

$$p(t|e_{s_i}, e_{o_i}, e_{p_i}, \mathcal{G}_{t_{i-1}}, \mathcal{G}_{t_{i-2}}, \dots, \mathcal{G}_1) = p(t|e_{s_i}, e_{o_i}, e_{p_i}, e_i^{h,sp}, e_i^{h,op}). \quad (9)$$

4.2 Neighborhood Aggregation

Because a subject entity can form links with multiple object entities within the same time slice, we use a mean aggregation module (Hamilton et al., 2017) to extract neighborhood information from concurrent events of a relevant historical event sequence. For predicting the missing object entity in the object prediction query $(e_{s_i}, e_{p_i}, ?, t_i)$, this module takes the element-wise mean of the embedding vectors of object entities in $\mathbf{O}_{t_j}(e_{s_i}, e_{p_i})$:

$$g(\mathbf{O}_{t_j}(e_{s_i}, e_{p_i})) = \frac{1}{|\mathbf{O}_{t_j}(e_{s_i}, e_{p_i})|} \sum_{e_o \in \mathbf{O}_{t_j}(e_{s_i}, e_{p_i})} \mathbf{e}_o \quad (10)$$

where we denote the mean aggregation of embeddings of the neighboring object entities as $g(\mathbf{O}_{t_j}(e_{s_i}, e_{p_i}))$.

4.3 The Graph Hawkes Process

By considering each timestamped edge of a temporal knowledge graph as an event between two nodes, we can represent a temporal knowledge graph as a continuous-time event sequence. The time span between events often has significant implications on the underlying intricate temporal dependencies. Therefore, we model time as a random variable and deploy the Hawkes process on temporal knowledge graphs to capture the underlying dynamics and name it as the Graph Hawkes Process. In contrast to the classic Hawkes process with a parametric form, we use a recurrent neural network to estimate the intensity function of the graph Hawkes process. Traditionally, recurrent neural networks are employed to synchronized series with evenly spaced intervals. However, events in a temporal KG have non-equal distant timestamps, which are asynchronously and randomly distributed over the continuous time space. Thus, inspired by the neural Hawkes process (Mei & Eisner, 2017) we use a continuous-time LSTM with an explicit time-dependent hidden state, where the hidden state is instantaneously updated with each event occurrence and also continuously evolves as time elapses between two neighbored events. Specifically, given an object prediction query $(e_{s_i}, e_{p_i}, ?, t_i)$ and its relevant historical event sequence $e_i^{h,sp}$, we define the intensity function of an object candidate e_o as follows:

$$\lambda(e_o|e_{s_i}, e_{p_i}, t_i, e_i^{h,sp}) = f(\mathbf{W}_\lambda(\mathbf{e}_{s_i} \oplus \mathbf{h}(e_o, e_{s_i}, e_{p_i}, t_i, e_i^{h,sp}) \oplus \mathbf{e}_{p_i}) \cdot \mathbf{e}_o) \quad (11)$$

where $\mathbf{e}_{s_i}, \mathbf{e}_{p_i}, \mathbf{e}_o \in \mathbb{R}^r$ (r denotes the rank of embeddings) are embedding vectors of the subject e_{s_i} , predicate e_{p_i} and object e_{o_i} of the event e_i , $\mathbf{h}(e_o, e_{s_i}, e_{p_i}, t_i, e_i^{h,sp}) \in \mathbb{R}^d$ (d represents the number of hidden dimensions) denotes the hidden state of a continuous-time recurrent neural network that takes $e_i^{h,sp}$ as input and summarizes information in the relevant historical event sequence, and \oplus represents the concatenation operator. We concatenate the subject entity embedding and the predicate embedding with the hidden state vector to let the model capture important information from the subject-predicate pair since it is the most important information we can get from an object prediction query $(e_{s_i}, e_{p_i}, ?, t_i)$. $\mathbf{W}_\lambda \in \mathbb{R}^{(2r+d) \times r}$ is the weight matrix of a linear layer for converting the dimensionality of the concatenation from $2r + d$ to r so that we can make a dot-product between it and the embedding of the object candidate e_o so that the network can capture the compatibility of the subject e_{s_i} and the object candidate e_o considering their previous interactions. This accounts for the behavior that entities tend to form relationships with other entities that have similar recent actions and goals (Trivedi et al., 2017).

Besides, the sign of each element of the hidden state vector $\mathbf{h}(e_o, e_{s_i}, e_{p_i}, t_i, e_i^{h,sp})$ can be both positive and negative. However, all elements of the intensity vector $\lambda(e_o|e_{s_i}, e_{p_i}, t_i, e_i^{h,sp})$ should be strictly positive defined at all timestamps when an event could possibly occur. Thus we need an activation function $f(x)$ so that each element of the intensity vector can meet our requirement. A

commonly used activation function is the Rectified Linear Units function. However, for a negative input x , we get zero back so that the output is not strictly positive. The softplus function gained attention in recent works (Mei & Eisner, 2017; Trivedi et al., 2018), which is a better choice. The softplus function is defined as:

$$f^{softplus}(x) = \log(1 + \exp(x)) \quad (12)$$

whose output value is strictly positive and approaches the ReLU function as the input x is far from zero. To make sure that the output values that are near to zero are also similar to the output of the ReLU function, Mei & Eisner (2017) introduced a scale parameter $s > 0$ for controlling the function’s curvature and defined a scaled softplus function:

$$f_{scaled}^{softplus}(x) = s \log(1 + \exp(x/s)). \quad (13)$$

All output values of the scaled softplus function are strictly positive defined and approach the corresponding outputs of the ReLU function as the scale parameter approaches to zero.

Similarly, given a subject prediction query $(?, e_{p_i}, e_{o_i}, t_i)$ and its relevant historical event sequence $e_i^{h,op}$, the intensity function of an subject candidate is defined as follows:

$$\begin{aligned} & \lambda(e_s | e_{p_i}, e_{o_i}, t_i, e_i^{h,op}) \\ &= f(\mathbf{W}_\lambda(\mathbf{e}_{o_i} \oplus \mathbf{h}(e_s, e_{p_i}, e_{o_i}, t_i, e_i^{h,op}) \oplus \mathbf{e}_{p_i}) \cdot \mathbf{e}_s) \end{aligned} \quad (14)$$

In the following, we take the $\mathbf{h}(e_o, e_{s_i}, e_{p_i}, t_i, e_i^{h,sp})$ as an example to show how the continuous-time LSTM works. Given an object entity query $(e_{s_i}, e_{p_i}, ?, t_i)$ and its relevant historical event sequence $e_i^{h,sp}$, we list the core functions of the continuous-time LSTM (Mei & Eisner, 2017) in the following:

$$\mathbf{k}_m = g(\mathbf{O}_{t_m}(e_{s_i}, e_{p_i})) \oplus \mathbf{e}_{s_i} \oplus \mathbf{e}_{p_i} \quad (15)$$

$$\mathbf{i}_{m+1} = \sigma(\mathbf{W}_i \mathbf{k}_m + \mathbf{U}_i \mathbf{h}(t_m) + d_i) \quad (16)$$

$$\bar{\mathbf{i}}_{m+1} = \sigma(\mathbf{W}_{\bar{i}} \mathbf{k}_m + \mathbf{U}_{\bar{i}} \mathbf{h}(t_m) + d_{\bar{i}}) \quad (17)$$

$$\mathbf{f}_{m+1} = \sigma(\mathbf{W}_f \mathbf{k}_m + \mathbf{U}_f \mathbf{h}(t_m) + d_f) \quad (18)$$

$$\bar{\mathbf{f}}_{m+1} = \sigma(\mathbf{W}_{\bar{f}} \mathbf{k}_m + \mathbf{U}_{\bar{f}} \mathbf{h}(t_m) + d_{\bar{f}}) \quad (19)$$

$$\mathbf{z}_{m+1} = \sigma(\mathbf{W}_z \mathbf{k}_m + \mathbf{U}_z \mathbf{h}(t_m) + d_z) \quad (20)$$

$$\mathbf{o}_{m+1} = \sigma(\mathbf{W}_o \mathbf{k}_m + \mathbf{U}_o \mathbf{h}(t_m) + d_o) \quad (21)$$

$$\mathbf{c}_{m+1} = \mathbf{f}_{m+1} \cdot \mathbf{c}(t_m) + \mathbf{i}_{m+1} \cdot \mathbf{z}_{m+1} \quad (22)$$

$$\bar{\mathbf{c}}_{m+1} = \bar{\mathbf{f}}_{m+1} \cdot \bar{\mathbf{c}}_m + \bar{\mathbf{i}}_{m+1} \cdot \mathbf{z}_{m+1} \quad (23)$$

$$\delta_{m+1} = f(\mathbf{W}_d \mathbf{k}_m + \mathbf{U}_d \mathbf{h}(t_m) + d_d) \quad \text{where } f(x) = \psi \log(1 + \exp(x/\psi)) \quad (24)$$

$$\mathbf{c}(t) = \bar{\mathbf{c}}_{m+1} + (\mathbf{c}_{m+1} - \bar{\mathbf{c}}_{m+1}) \exp(-\delta_{m+1}(t - t_m)) \quad (25)$$

Here, \mathbf{k} denotes the input vector; \mathbf{f} , \mathbf{i} , \mathbf{o} , \mathbf{z} , and \mathbf{c} denotes the forget gate, input gate, output gate, cell update, and discrete cell, respectively; $\mathbf{c}(t)$ represents the continuous-time cell function, $\bar{\mathbf{i}}$ and $\bar{\mathbf{f}}$ are additional gates for computing the continuous-time cell; $\bar{\mathbf{c}}$ represents the target cell state; and δ denotes the decaying function. At a timestamp t_m , we feed the input \mathbf{k}_m into the network and update gate functions and memory cells. For capturing cumulative knowledge in the historical event sequence, the input \mathbf{k}_m concatenates the neighborhood aggregation based on $\mathbf{O}_{t_m}(e_{s_i}, e_{p_i})$ with the embedding vector of the corresponding subject entity e_{s_i} and predicate e_{p_i} as the input of continuous-time LSTM. Formulas 16, 18, 20, 21 and 22 are as same as the gates and the cell in the discrete-time LSTM (Graves, 2013) while the gate functions 19 and 17 are designed to formulate Equation 23 that characterizes the target cell state that the continuous-time cell function approaches to between two update timestamps t_m and t_{m+1} . Equation 24 defines how the continuous-time cell function approaches to a target cell state $\bar{\mathbf{c}}_{m+1}$ from an initial cell state \mathbf{c}_{m+1} as the time continue to vary. Thus, The formulas from 17 to 24 listed above make a discrete update to each state and gate function. Noticeably, the update does not depend on the hidden state of the last update $\mathbf{h}(t_{m-1})$ but rather the value $\mathbf{h}(t_m)$ at timestamp t_m .

Equations 25 makes the cell function $\mathbf{c}(t)$ instantaneously jump to a initial cell state \mathbf{c}_{m+1} at each update of the cLSTM and then continuously drift toward a target cell state $\bar{\mathbf{c}}_{m+1}$, which in turn

controls the hidden state vector as well as the intensity function. Thus, between two update timestamps $(t_m, t_{m+1}]$, $\mathbf{c}(t)$ follows an exponential curve to approach the target cell state. Equation 26 describes how $\mathbf{c}(t)$ controls the hidden state vector $\mathbf{h}(e_o, e_{s_i}, e_{p_i}, t, e_i^{h,sp})$ that is analogous to h_m in a discrete-time LSTM model that extracts relevant information from the past event sequence. However, in the architecture of the continuous-time LSTM (Mei & Eisner, 2017), it will also reflect the interarrival times $t_1 - 0, t_2 - t_1, \dots, t_{m+1} - t_m$. The interval $(t_m, t_{m+1}]$ ends when the next event happens at some time t_{m+1} , where the continuous-time LSTM takes $\mathbf{O}_{t_{m+1}}(e_{s_i}, e_{p_i})$ as the input and update the current memory cell $\mathbf{c}(t)$ to new initial value \mathbf{c}_{m+1} based on the hidden state at the timestamp t_{m+1} . Additionally, the term $\mathbf{c}_{m+1} - \bar{\mathbf{c}}_{m+1}$ is related to the degree to which the past relevant events influence the current events; the influence on the elements of the vector $\mathbf{c}(t)$ could be either excitatory or inhibitory, depending on the sign of the corresponding element of the decaying vector δ_{m+1} .

$$\mathbf{h}(e_o, e_{s_i}, e_{p_i}, t, e_i^{h,sp}) = \mathbf{e}_{o_i} \cdot \tanh(\mathbf{c}(t)) \quad \text{for } t \in (t_m, t_{m+1}] \quad (26)$$

The hidden state $\mathbf{h}(e_o, e_{s_i}, e_{p_i}, t_i, e_i^{h,sp})$ reflects how the system’s expectations about the next occurrence of a specific triplet change as time elapses and models the structural and temporal coherence in the given temporal knowledge graph. This is because, first, the hidden state $\mathbf{h}(e_o, e_{s_i}, e_{p_i}, t_i, e_i^{h,sp})$ summarizes historical information of the subject entity e_{s_i} involved in the query and the edges it created in the past. This information is utilized for computing the compatibility of the subject entity e_{s_i} and candidates for the missing object entity. Again, this accounts for the behavior that entities tend to form edges with other entities that have similar recent interactions. Thus, this recurrent architecture is able to use historical information to model the intricate non-linear and evolving dynamics of the given temporal knowledge graph.

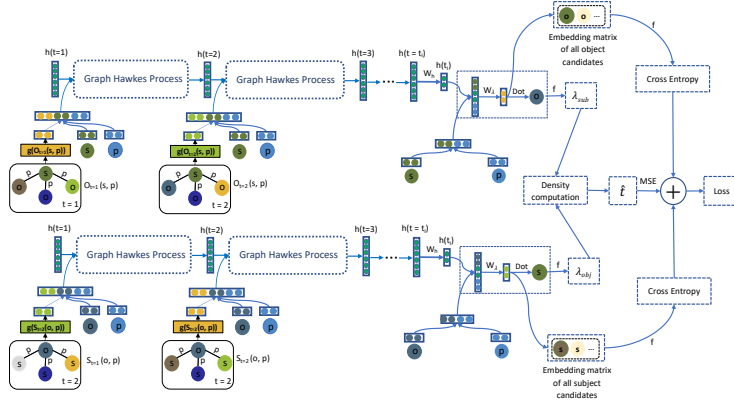


Figure 2: Visualization of the Graph Hawkes Network Architecture. Here we focus on a specific training quadruple $(e_{s_i}, e_{p_i}, e_{o_i}, t_i)$, where the embeddings of e_{s_i} , e_{p_i} , and e_{o_i} are represented as green nodes, blue nodes and cyan nodes, respectively. $h(t)$ stands for hidden vector in the cLSTM. f is the scaled soft-plus function where $f(x) = \psi \log(1 + \exp(x/\psi))$. The Graph Hawkes Network uses the neighborhood aggregation and the Graph Hawkes Process to summarize interactions between subject entity e_{s_i} and object entities in \mathbf{O}_t as well as interactions between object entity e_{o_i} with subject entities in \mathbf{S}_t at different timestamps, and derives an intensity function of the quadruple for prediction tasks.

4.4 Inference and Parameter Learning

In this section, we will provide details about how the Graph Hawkes Network perform inference for the link prediction task and the time prediction task. Additionally, we will introduce the training procedure of the Graph Hawkes Network.

Link prediction Given a object prediction query $(e_{s_i}, e_{p_i}, ?, t_i)$ and its relevant historical event sequence $e_i^{h,sp}$, we derive the conditional density function of an object candidate e_o from Equation

2, which gives the following equation:

$$\begin{aligned} p(e_o|e_{s_i}, e_{p_i}, t_i, e_i^{h,sp}) \\ = \lambda(e_o|e_{s_i}, e_{p_i}, t_i, e_i^{h,sp}) \exp\left(-\int_{t_L}^{t_i} \lambda_{surv}(e_{s_i}, e_{p_i}, \tau) d\tau\right) \end{aligned} \quad (27)$$

where t_L denotes the timestamp of the most recent historical event in $e_i^{h,sp}$, and $\int_{t_L}^t \lambda_{surv}(e_{s_i}, e_{p_i}, \tau) d\tau$ is the survival term (Daley & Vere-Jones, 2007) of all possible events $\{e_{s_i}, e_{p_i}, e_o = j\}_{j=1}^{N_e}$ with regarding to the given subject entity e_{s_i} and the predicate e_{p_i} , which is defined as:

$$\lambda_{surv}(e_{s_i}, e_{p_i}, t) = \sum_{e_o=1}^{N_e} \lambda_{sub}(e_{s_i}, e_{p_i}, e_o, t) \quad (28)$$

that penalizes non-presence of these events in a given observation window (Trivedi et al., 2017). We see that all object candidates share the same survival term $\lambda_{surv}(e_{s_i}, e_{p_i}, t)$ and the same value of t_L , the corresponding conditional density functions also have the same integral in Equation 27. Thus, instead of comparing the conditional density function of each object candidate e_o , we can directly compare their intensity function $\lambda(e_o|e_{s_i}, e_{p_i}, t_i, e_i^{h,sp})$ to avoid the computationally expensive integral calculations. We then sort all the candidates in the descending order of this density to rank the correct entity for the object position.

Time prediction For the time prediction task, given an event $(e_{s_i}, e_{p_i}, e_{o_i})$, we aim to predict the expected value of its next happening time based on observed events. Since we have full information about the involving subject entity and the object entity, we can utilize both $e_i^{h,sp}$ and $e_i^{h,op}$. Hence, the intensity that an event type $(e_{s_i}, e_{p_i}, e_{o_i})$ occurs at a future time is defined as follows:

$$\begin{aligned} \lambda(t|e_{s_i}, e_{p_i}, e_{o_i}, e_i^{h,sp}, e_i^{h,op}) = & \int_{scaled}^{softplus} (\mathbf{W}_\lambda(\mathbf{e}_{s_i} \oplus \mathbf{h}(e_{o_i}, e_{s_i}, e_{p_i}, t_i, e_i^{h,sp}) \oplus \mathbf{e}_{p_i}) \cdot \mathbf{e}_{o_i}) \\ & + \int_{scaled}^{softplus} (\mathbf{W}_\lambda(\mathbf{e}_{o_i} \oplus \mathbf{h}(e_{s_i}, e_{o_i}, e_{p_i}, t_i, e_i^{h,op}) \oplus \mathbf{e}_{p_i}) \cdot \mathbf{e}_{s_i}) \end{aligned} \quad (29)$$

Normally, the Hawkes process predicts when the next event will happen without regarding the event type. In contrast, our task here is to predict the next happening time of the given event type $(e_{s_i}, e_{p_i}, e_{o_i})$. Thus, we consider it as a Hawkes process with a single event type¹. This gives the corresponding conditional density function:

$$\begin{aligned} p(t|e_{s_i}, e_{p_i}, e_{o_i}, e_i^{h,sp}, e_i^{h,op}) \\ = \lambda(t|e_{s_i}, e_{p_i}, e_{o_i}, e_i^{h,sp}, e_i^{h,op}) \exp\left(-\int_{t_L}^t \lambda(\tau|e_{s_i}, e_{p_i}, e_{o_i}, e_i^{h,sp}, e_i^{h,op}) d\tau\right) \end{aligned} \quad (30)$$

Accordingly, the expectation of the next event time is computed by:

$$\hat{t}_i = \int_{t_L}^{\infty} t \cdot p(t|e_{s_i}, e_{p_i}, e_{o_i}, e_i^{h,sp}, e_i^{h,op}) dt \quad (31)$$

where the integrals in the preceding equations can be estimated by Monte Carlo sampling.

Parameter learning Because the link prediction can be viewed as a multi-class classification task, where each class corresponds to an entity candidate, we use the cross-entropy loss for learning the link prediction:

$$\mathcal{L}_{link}^{sp} = -\sum_{i=1}^N \sum_{c=1}^{N_e} y_c \log(p(e_{o_i} = c|e_{s_i}, e_{p_i}, t_i, e_i^{h,sp})) \quad (32)$$

$$\mathcal{L}_{link}^{op} = -\sum_{i=1}^N \sum_{c=1}^{N_e} y_c \log(p(e_{s_i} = c|e_{o_i}, e_{p_i}, t_i, e_i^{h,op})) \quad (33)$$

where \mathcal{L}_{link}^{sp} is the loss of object prediction given the query $(e_{s_i}, e_{p_i}, ?, t_i)$ and \mathcal{L}_{link}^{op} is the loss of subject prediction given the query $(?, e_{p_i}, e_{o_i}, t_i)$, and y_c is a binary indicator of whether class label

¹It can be easily derived from the Equation 2 that the integration of the density function of the Hawkes process with a single event type is one.

c is the correct classification for predicting e_{o_i} and e_{s_i} . Besides, since timestamps are not discrete labels, we use the mean square error as the time prediction loss:

$$\mathcal{L}_{\text{time}} = \sum_{i=1}^N (t_i - \hat{t}_i)^2 \quad (34)$$

Hence, the total loss is the sum of the time prediction loss and the link prediction loss:

$$\mathcal{L} = \mathcal{L}_{\text{link}}^{\text{sp}} + \mathcal{L}_{\text{link}}^{\text{op}} + w\mathcal{L}_{\text{time}} \quad (35)$$

Additionally, we balance the loss of the time prediction task and the loss of the link prediction task by scaling the former using a hyperparameter w . The learning algorithm of the Graph Hawkes Network is described in the Appendix A. Also, we illustrated the architecture of the Graph Hawkes Network in the Figure 2.

Table 1: Statistics of the GDELT15/16 dataset and the ICEWS14 dataset.

Dataset Name	# Entities	# Predicates	# Quadruples	# Timestamps
GDELT15/16	7398	239	1.97M	2591
ICEWS14	12498	254	0.49M	269

Table 2: Link prediction results: MRR (%) and Hits@1/3/10 (%).

Datasets	ICEWS14 - filtered				GDELT15/16 - filtered			
Metrics	MRR	Hits@1	Hits@3	Hits@10	MRR	Hits@1	Hits@3	Hits@10
T-TransE	7.15	1.39	6.91	18.93	5.45	0.44	4.89	15.10
TA-TransE	11.35	0.00	15.23	34.25	9.57	0.00	12.51	27.91
TA-Dismult	10.73	4.86	10.86	22.52	10.28	4.87	10.29	20.43
LiTSEE	6.45	0.00	7.00	19.40	6.64	0.00	8.10	18.72
Know-Evolve ^a	1.42	1.35	1.37	1.43	2.43	2.33	2.35	2.41
Re-Net	28.56	18.74	31.49	48.54	22.24	14.24	23.95	38.21
GHN	28.67 \pm 0.038	19.75 \pm 0.060	31.60 \pm 0.020	46.50 \pm 0.025	23.55 \pm 0.023	15.66 \pm 0.032	25.51 \pm 0.015	38.92 \pm 0.036

^aThere is a flaw in the original evaluation sourcecode of Know-Evolve. Its performance dramatically drops when using newly defined ranking metric described in Section 5.1.

Table 3: Time prediction results: MAE and cHits@1/3/10 (%).

Datasets	ICEWS14 - filtered			GDELT15/16 - filtered		
Metrics	MAE (days)	cHits@1	cHits@10	MAE (hours)	cHits@1	cHits@10
Know-Evolve ²	1.78	-	-	110.5	-	-
LiTSEE	108.00	-	25.10	303.78	-	0.00
GHN	4.37 \pm 0.012	70.48 \pm 0.035	92.79 \pm 0.030	4.66 \pm 0.008	61.29 \pm 0.061	91.17 \pm 0.104

5 Experiments

5.1 Experimental Setup

Datasets Global Database of Events, Language, and Tone (GDELT) (Leetaru & Schrodtt, 2013) dataset and Integrated Crisis Early Warning System (ICEWS) (Boschee et al., 2015) dataset have been drawing attention in the community as representative samples of tKGs (Schein et al., 2016). The

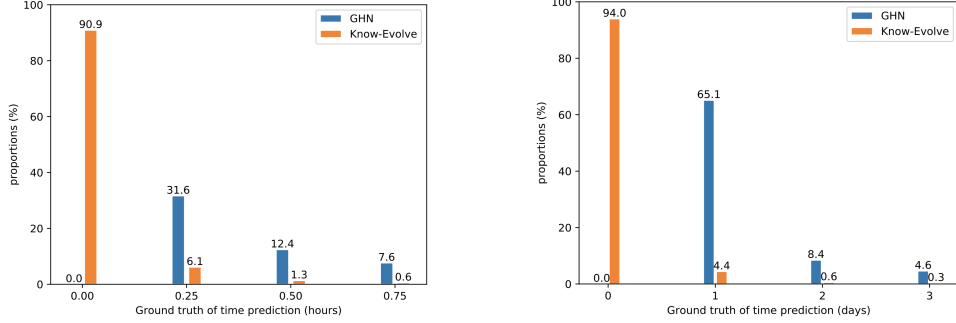


Figure 3: Ground truth of the time prediction task in the GDELDT dataset (the left figure) and the ICEWS14 dataset (the right figure) with regarding to the settings in Know-Evolve and in GHN. The orange bars represent the proportions of each ground truth value in Know-Evolve while the blue bars represent the proportions of each ground truth value in GHN. Here we can see that the most ground truth values in Know-Evolve are zeros, leading to the fact that Know-Evolve can easily learn the statistics and have high hits@ k value for the time prediction task.

GDELDT dataset is an initiative to construct a database of all the events across the globe connecting people, organizations, events, news sources, and locations (Kazemi, Goel, Jain, et al., 2019). We use a subset (GDELDT15/16) of the GDELDT dataset, which contains events occurring from April 1, 2015 to March 31, 2016. The ICEWS dataset contains information about political events with specific time annotations, e.g. (Ban Ki-moon, Secretary-General of, the United Nations). We apply our model on a subset (ICEWS14) of the ICEWS dataset, which contains events in 2014. The statistics of the datasets are provided in Table 1. We compare our approach and some baseline methods by performing the link prediction task as well as the time prediction task on the GDELDT15/16 dataset and the ICEWS14 dataset. Table 1 provides statistics about the experimental datasets.

Implementation details of the GHN By training the Graph Hawkes Network, we set the maximal length of historical event sequences to be 10, the size of embeddings of entities/predicates to be 200, and the learning rate to be 0.001. The model is trained by the Adam optimizer. We set the weight decay rate to be 0.00001, and the batch size to be 1024. The above configurations were used for all experiments that were done on GeForce GTX 1080 Ti.

Evaluation metrics There are different metrics for evaluating the results of the link prediction. The the mean reciprocal rank (MRR) is one of those commonly used evaluation metrics, where we remove an entity (subject or object) in a test triplet, replaced by all entities that can potentially be the missing entity, then find the rank of the actual missing entity, and then take the reciprocal value. Besides, some researchers often use Hits@K to evaluate the performance of models, which is the percentage that the actual missing entity is ranked in the top K. However, these metrics can be flawed when some corrupted triplets end up being valid ones, from the training set for instance (Bordes et al., 2013). In this case, those may be ranked above the actual missing entity, but this should not be seen as an error because both triplets are true. To avoid such a misleading behavior, Bordes et al. (2013) suggested to remove from the list of corrupted triplets all the triplets that appear either in the training, validation, or test set except the test triplet of interest. This ensures that all corrupted triplets do not belong to the dataset.

The ranking technique described in (Bordes et al., 2013) is reasonable for evaluating the link prediction over semantic knowledge graphs; however, we think it is not appropriate for temporal knowledge graphs since a temporal fact is only valid at some timestamps. Therefore, we define a new ranking procedure. For a test quadruple $(e_{s_i}, e_{p_i}, ?, t_i)$, instead of removing from the list of corrupted triplets all the triplets that appear either in the training, validation or test set, we only filter from the list all the triplets that occur at t_i . This ensures that the facts that do not appear at t_i are still considered as corrupted triplets for evaluating the given quadruple. Additionally, since all object candidates are ranked by their scores, some entities may have the same scores. In this case, most literature gives the highest rank (first rank) for all entities, leading that the rank may be incredibly high even if the estimator has an unconfident prediction. For a fair evaluation, we give a mean rank to entities that have the same scores (Jin et al., 2019).

For the time prediction task, Trivedi et al. (2017) used the mean absolute error (MAE) between the predicted time and the ground truth to evaluate the experiment results. However, a small part of bad predictions may lead to high MAE although the majority of predictions has good quality. Thus, we propose the continuous Hits@ k (cHits@ k) for the time prediction task where cHits@ k is defined as the ratio of data samples whose MAE is smaller than k .

For each dataset, we report Mean Reciprocal Ranks (MRR) and Hits@ k for the link prediction task; we also report Mean Absolute Error (MAE) and cHits@ k for the time prediction task.

Baseline methods For the link prediction task, we compare the performance of our model with several state-of-the-art methods for tKGs, including TTransE (Leblay & Chekol, 2018), TA-TransE/DistMult (García-Durán et al., 2018), Know-Evolve (Trivedi et al., 2017), and RE-Net (Jin et al., 2019). For the time prediction task, we compare our model only with AiTSEE (Xu et al., 2019) and Know-Evolve since only these two models are capable of performing the time prediction task on tKGs to the best of our knowledge.

We use our newly defined ranking metrics to evaluate all baseline models. We implement TTransE, TA-TransE, and TA-DistMult based on the implementation provided in (Jin et al., 2019). We use the Adam optimizer to train the baseline models and optimize hyperparameters by early validation stopping according to MRR on the validation set. We set the iterations to 1000, the batch size to 1024, the margin to 1.0, and the negative sample ratio to 1. We implement LiTSEE based on the implementation of TransE (Bordes et al., 2013). We implement KnowEvolve in PyTorch based on the sourcecode³. We use the sourcecode for RE-Net⁴. We keep the default settings of hyperparameters.

5.2 Performance Comparison on Temporal Knowledge Graphs

Link prediction results Table 2 summarizes link prediction performance comparison on both datasets. GHN gives on-par results with RE-Net and outperforms all other models on these datasets considering MRR, Hits@1, and Hits@3. Know-Evolve shows poor performance when using our newly defined ranking metric due to its limited capability of dealing with concurrent events. Additionally, our model beats RE-Net because they only consider the order of relevant historical events. However, GHN explicitly encodes time information into the intensity function, which improves the expressivity of our model. These results prove that the Graph Hawkes Process substantially enhances the performance of reasoning on tKGs.

Time prediction results Table 3 demonstrates that GHN performs significantly better than LiTSEE for the time prediction task on the ICEWS14 dataset and the GDELT15/16 dataset. This result shows the superiority of the GHN compared to methods that model tKGs by merely adding a temporal component into entity embeddings. Furthermore, Know-Evolve has good results on the ICEWS14 dataset due to its simplest ground truth distribution. As shown in Figure 3, the most ground-truth values in the ICEWS14 dataset as well as in the GDELT15/16 dataset for the time prediction task are exactly zero according to the settings in Know-Evolve. The reason is that, for a given triple (e_s, e_p, e_o) , Know-Evolve chooses the latest interaction time of either e_s or e_o as the reference time point for predicting the next event time and processes the data sequentially without considering concurrent events. Thus, compared to GHN, Know-Evolve cannot make long-term predictions since it only predicts t_i at latest interaction time of either e_{s_i} or e_{o_i} , which is very near to t_i .

6 Conclusion

We presented the Graph Hawkes Network, a novel neural architecture for reasoning about temporal knowledge graphs. To model the temporal dynamics of tKGs, we utilized the Graph Hawkes Process, a multivariate point process model of streams of timestamped events, that can capture underlying dynamics across facts. The model parameters are learned via a continuous-time recurrent neural network (LSTM), which is able to estimate the probability of events at an arbitrary timestamp. We test our model on temporal knowledge graphs, where experimental results demonstrate that our approach outperforms the state-of-the-art methods on link prediction and time prediction over tKGs.

³<https://github.com/rstriv/Know-Evolve>

⁴<https://github.com/INK-USC/RE-Net>

References

- Aalen, O., Borgan, O., & Gjessing, H. (2008). *Survival and event history analysis: a process point of view*. Springer Science & Business Media.
- Bacry, E., Jaisson, T., & Muzy, J.-F. (2016). Estimation of slowly decreasing hawkes kernels: application to high-frequency order book dynamics. *Quantitative Finance*, 16(8), 1179–1201.
- Bordes, A., Usunier, N., Garcia-Duran, A., Weston, J., & Yakhnenko, O. (2013). Translating embeddings for modeling multi-relational data. In *Advances in neural information processing systems* (pp. 2787–2795).
- Boschee, E., Lautenschlager, J., O’Brien, S., Shellman, S., Starz, J., & Ward, M. (2015). Iccws coded event data. *Harvard Dataverse*, 12.
- Carlson, A., Betteridge, J., Kisiel, B., Settles, B., Hruschka, E. R., & Mitchell, T. M. (2010). Toward an architecture for never-ending language learning. In *Twenty-fourth aaai conference on artificial intelligence*.
- Daley, D. J., & Vere-Jones, D. (2007). *An introduction to the theory of point processes: volume ii: general theory and structure*. Springer Science & Business Media.
- Dasgupta, S. S., Ray, S. N., & Talukdar, P. (2018). Hyte: Hyperplane-based temporally aware knowledge graph embedding. In *Proceedings of the 2018 conference on empirical methods in natural language processing* (pp. 2001–2011).
- Du, N., Dai, H., Trivedi, R., Upadhyay, U., Gomez-Rodriguez, M., & Song, L. (2016). Recurrent marked temporal point processes: Embedding event history to vector. In *Proceedings of the 22nd acm sigkdd international conference on knowledge discovery and data mining* (pp. 1555–1564).
- Esteban, C., Tresp, V., Yang, Y., Baier, S., & Krompaß, D. (2016). Predicting the co-evolution of event and knowledge graphs. In *2016 19th international conference on information fusion (fusion)* (pp. 98–105).
- García-Durán, A., Dumančić, S., & Niepert, M. (2018). Learning sequence encoders for temporal knowledge graph completion. *arXiv preprint arXiv:1809.03202*.
- Graves, A. (2013). Generating sequences with recurrent neural networks. *arXiv preprint arXiv:1308.0850*.
- Hamilton, W., Ying, Z., & Leskovec, J. (2017). Inductive representation learning on large graphs. In *Advances in neural information processing systems* (pp. 1024–1034).
- Hawkes, A. G. (1971). Spectra of some self-exciting and mutually exciting point processes. *Biometrika*, 58(1), 83–90.
- Jiang, T., Liu, T., Ge, T., Sha, L., Chang, B., Li, S., & Sui, Z. (2016). Towards time-aware knowledge graph completion. In *Proceedings of coling 2016, the 26th international conference on computational linguistics: Technical papers* (pp. 1715–1724).
- Jin, W., Zhang, C., Szekely, P., & Ren, X. (2019). Recurrent event network for reasoning over temporal knowledge graphs. *arXiv preprint arXiv:1904.05530*.
- Kazemi, S. M., Goel, R., Eghbali, S., Ramanan, J., Sahota, J., Thakur, S., . . . Brubaker, M. (2019). Time2vec: Learning a vector representation of time. *arXiv preprint arXiv:1907.05321*.
- Kazemi, S. M., Goel, R., Jain, K., Kobayez, I., Sethi, A., Forsyth, P., & Poupart, P. (2019). Relational representation learning for dynamic (knowledge) graphs: A survey. *arXiv preprint arXiv:1905.11485*.

- Leblay, J., & Chekol, M. W. (2018). Deriving validity time in knowledge graph. In *Companion proceedings of the the web conference 2018* (pp. 1771–1776).
- Leetaru, K., & Schrod, P. A. (2013). Gdelt: Global data on events, location, and tone, 1979–2012. In *Isa annual convention* (Vol. 2, pp. 1–49).
- Lin, Y., Liu, Z., Sun, M., Liu, Y., & Zhu, X. (2015). Learning entity and relation embeddings for knowledge graph completion. In *Twenty-ninth aaai conference on artificial intelligence*.
- Liu, W., & Lü, L. (2010, 01). Link prediction based on local random walk. *Europhysic Letter*, 89. doi: 10.1209/0295-5075/89/58007
- Ma, Y., Tresp, V., & Daxberger, E. A. (2018). Embedding models for episodic knowledge graphs. *Journal of Web Semantics*, 100490.
- Mei, H., & Eisner, J. M. (2017). The neural hawkes process: A neurally self-modulating multivariate point process. In *Advances in neural information processing systems* (pp. 6754–6764).
- Minervini, P., d’Amato, C., Fanizzi, N., & Tresp, V. (2014). Learning to propagate knowledge in web ontologies. In *Ursw* (pp. 13–24).
- Nickel, M., Tresp, V., & Kriegel, H.-P. (2011). A three-way model for collective learning on multi-relational data. In *Icml* (Vol. 11, pp. 809–816).
- Ogata, Y. (1998). Space-time point-process models for earthquake occurrences. *Annals of the Institute of Statistical Mathematics*, 50(2), 379–402.
- Palm, C. (1943). *Intensitätsschwankungen im fernsprechverkehr* (No. 44). Ericsson technics. Retrieved from <https://books.google.com/books?id=5cy2NQAACAAJ>
- Sankar, A., Wu, Y., Gou, L., Zhang, W., & Yang, H. (2018). Dynamic graph representation learning via self-attention networks. *arXiv preprint arXiv:1812.09430*.
- Schein, A., Zhou, M., Blei, D. M., & Wallach, H. (2016). Bayesian poisson tucker decomposition for learning the structure of international relations. *arXiv preprint arXiv:1606.01855*.
- Schlichtkrull, M., Kipf, T. N., Bloem, P., Van Den Berg, R., Titov, I., & Welling, M. (2018). Modeling relational data with graph convolutional networks. In *European semantic web conference* (pp. 593–607).
- Singhal, A. (2012). Introducing the knowledge graph: things, not strings. *Official google blog*, 5.
- Trivedi, R., Dai, H., Wang, Y., & Song, L. (2017). Know-evolve: Deep temporal reasoning for dynamic knowledge graphs. In *Proceedings of the 34th international conference on machine learning* (Vol. 70, pp. 3462–3471).
- Trivedi, R., Farajtabar, M., Biswal, P., & Zha, H. (2018). Dyrep: Learning representations over dynamic graphs.
- Trouillon, T., Dance, C. R., Gaussier, É., Welbl, J., Riedel, S., & Bouchard, G. (2017). Knowledge graph completion via complex tensor factorization. *The Journal of Machine Learning Research*, 18(1), 4735–4772.
- Wang, Z., Zhang, J., Feng, J., & Chen, Z. (2014). Knowledge graph embedding by translating on hyperplanes. In *Twenty-eighth aaai conference on artificial intelligence*.
- Xu, C., Nanyeri, M., Alkhoury, F., Lehmann, J., & Yazdi, H. S. (2019). Temporal knowledge graph embedding model based on additive time series decomposition. *arXiv preprint arXiv:1911.07893*.
- Yang, B., Yih, W.-t., He, X., Gao, J., & Deng, L. (2014). Embedding entities and relations for learning and inference in knowledge bases. *arXiv preprint arXiv:1412.6575*.

A Parameter Learning

The learning algorithm of Graph Hawkes Network is described in the Algorithm 1. As mentioned in Section 4.2, we define the set of object entities interacting with a subject entity e_{s_i} under a predicate e_{p_i} at a timestamp t_j ($0 \leq t_j \leq t_i$) as $\mathbf{O}_{t_j}(e_{s_i}, e_{p_i})$. Similarly, we denote the set of subject entities interacted with the corresponding object entity and the predicate at t_j as $\mathbf{S}_{t_j}(e_{o_i}, e_{p_i})$. Additionally, this algorithm utilizes the cLSTM cell described in the Algorithm 2.

Algorithm 1: Learning parameters of the GHN.

Input : Sequence of training quadruples \mathbb{E} , entity set E , hyperparameter w , historical event sequences $e^{h,sp}$ and $e^{h,op}$.

Output : A trained network for the time prediction task and the link prediction task; embeddings for each entity and predicate.

while loss does not converge **do**

for $e_i = (e_{s_i}, e_{p_i}, e_{o_i}, t_i)$ in \mathbb{E} **do**

 Initialize the hidden state \mathbf{h}_{sub} , \mathbf{h}_{obj} with zero vector, $t_L = 0$.

for $e_i^{h,sp}[t_j]$ in $e_i^{h,sp}$ **do**

if $e_i^{h,sp}[t_j]$ is not a empty set **then**

$g(\mathbf{O}_{t_j}(e_{s_i}, e_{p_i})) = \frac{1}{|\mathbf{O}_{t_j}(e_{s_i}, e_{p_i})|} \sum_{e_o \in \mathbf{O}_{t_j}(e_{s_i}, e_{p_i})} \mathbf{e}_o$

$\mathbf{k}_j^{sub} = g(\mathbf{O}_{t_j}(e_{s_i}, e_{p_i})) \oplus \mathbf{e}_{s_i} \oplus \mathbf{e}_{p_i}$

$\mathbf{c}(t) \leftarrow \text{cLSTM_Cell}(\mathbf{k}_j^{sub}, \mathbf{h}_{sub}, c(t))$

$\mathbf{h}_{sub}(t) = \mathbf{e}_{o_i} \cdot \tanh(\mathbf{c}(t))$

$t_L = t_j$

end

end

for $e_i^{h,op}[t_j]$ in $e_i^{h,op}$ **do**

if $e_i^{h,op}[t_j]$ is not a empty set **then**

$g(\mathbf{S}_{t_j}(e_{o_i}, e_{p_i})) = \frac{1}{|\mathbf{S}_{t_j}(e_{o_i}, e_{p_i})|} \sum_{e_s \in \mathbf{S}_{t_j}(e_{o_i}, e_{p_i})} \mathbf{e}_s$

$\mathbf{k}_j^{obj} = g(\mathbf{S}_{t_j}(e_{o_i}, e_{p_i})) \oplus \mathbf{e}_{o_i} \oplus \mathbf{e}_{p_i}$

$\mathbf{c}(t) \leftarrow \text{cLSTM_Cell}(\mathbf{k}_j^{obj}, \mathbf{h}_{obj}, c(t))$

$\mathbf{h}_{obj}(t) = \mathbf{e}_{s_i} \cdot \tanh(\mathbf{c}(t))$

$t_L \leftarrow \max(t_L, t_j)$

end

end

$\lambda_{sub}(e_{s_i}, e_{p_i}, e_{o_i}, t, e_i^{h,sp}) = f(\mathbf{W}_\lambda(\mathbf{e}_{s_i} \oplus \mathbf{W}_h \mathbf{h}_{sub}(t) \oplus \mathbf{e}_{p_i}) \cdot \mathbf{e}_o)$

$\lambda_{obj}(e_{s_i}, e_{p_i}, e_{o_i}, t, e_i^{h,op}) = f(\mathbf{W}_\lambda(\mathbf{e}_{o_i} \oplus \mathbf{W}_h \mathbf{h}_{obj}(t) \oplus \mathbf{e}_{p_i}) \cdot \mathbf{e}_s)$

$\mathcal{L}_{link}(e_i) = -\log\left(\frac{\exp(\lambda_{sub}(e_{s_i}, e_{p_i}, e_{o_i}, t_i, e_i^{h,sp}))}{\sum_{o \in E} \exp(\lambda_{sub}(e_{s_i}, e_{p_i}, o, t_i, e_i^{h,sp}))} \cdot \frac{\exp(\lambda_{obj}(e_{s_i}, e_{p_i}, e_{o_i}, t_i, e_i^{h,op}))}{\sum_{s \in E} \exp(\lambda_{obj}(s, e_{p_i}, e_{o_i}, t_i, e_i^{h,op}))}\right)$

$\lambda_t(e_{s_i}, e_{p_i}, e_{o_i}, t, e_i^{h,sp}, e_i^{h,op}) = \frac{1}{2}(\lambda_{sub}(e_{s_i}, e_{p_i}, e_{o_i}, t, e_i^{h,sp}) + \lambda_{obj}(e_{s_i}, e_{p_i}, e_{o_i}, t, e_i^{h,op}))$

$p(t_i = t | e_{s_i}, e_{p_i}, e_{o_i}, e_i^{h,sp}, e_i^{h,op}) = \lambda_t(e_{s_i}, e_{p_i}, e_{o_i}, t) \exp(-\int_{t_L}^t \lambda_t(e_{s_i}, e_{p_i}, e_{o_i}, \tau) d\tau)$

$\mathcal{L}_{time}(e_i) = (t_i - \int_{t_L}^\infty t \cdot p(t | e_{s_i}, e_{p_i}, e_{o_i}, e_i^{h,sp}, e_i^{h,op}))^2$

$\mathcal{L}_{e_i} = \mathcal{L}_{link}(e_i) + w \mathcal{L}_{time}(e_i)$

end

$\mathcal{L} = \sum_{e_i \in \mathbb{E}} \mathcal{L}_{e_i}$

 Update model parameters.

end

Algorithm 2: A cell of feed-forward continuous-time LSTM

Input : Input vector $\mathbf{k}_i, \mathbf{h}(t_i), \mathbf{c}(t_i)$ **Output** : Memory cell $\mathbf{c}(t)$.

$$\begin{aligned}\mathbf{i}_{i+1} &= \sigma(\mathbf{W}_i \mathbf{k}_i + \mathbf{U}_i \mathbf{h}(t_i) + d_i) \\ \mathbf{f}_{i+1} &= \sigma(\mathbf{W}_f \mathbf{k}_i + \mathbf{U}_f \mathbf{h}(t_i) + d_f) \\ \mathbf{z}_{i+1} &= \sigma(\mathbf{W}_z \mathbf{k}_i + \mathbf{U}_z \mathbf{h}(t_i) + d_z) \\ \mathbf{o}_{i+1} &= \sigma(\mathbf{W}_o \mathbf{k}_i + \mathbf{U}_o \mathbf{h}(t_i) + d_o) \\ \mathbf{c}_{i+1} &= \mathbf{f}_{i+1} \cdot \mathbf{c}(t_i) + \mathbf{i}_{i+1} \cdot \mathbf{z}_{i+1} \\ \bar{\mathbf{c}}_{i+1} &= \bar{\mathbf{f}}_{i+1} \cdot \bar{\mathbf{c}}_i + \bar{\mathbf{i}}_{i+1} \cdot \bar{\mathbf{z}}_{i+1} \\ \delta_{i+1} &= f(\mathbf{W}_d \mathbf{k}_i + \mathbf{U}_d \mathbf{h}(t_i) + d_d) \text{ where } f(x) = \psi \log(1 + \exp(x/\psi)) \\ \mathbf{c}(t) &= \bar{\mathbf{c}}_{i+1} + (\mathbf{c}_{i+1} - \bar{\mathbf{c}}_{i+1}) \exp(-\delta_{i+1}(t - t_i)) \quad \text{for } t \in (t_i, t_{i+1}]\end{aligned}$$

B Comparison of the Hawkes Process with Other Point Processes

The Graph Hawkes Process is more stable than other intensity functions because its intensity function of each event type always approaches to its baseline rate. Taking Rayleigh Process as an example, its intensity function of an event type k is defined as follows (Trivedi et al., 2017):

$$\lambda_k(t) = \alpha_k \cdot t \quad (36)$$

where α_k is the weight parameter of the event type k . Thus, the intensities linearly increase with time, and therefore, it is not bounded. Moreover, although the linearity of the Rayleigh process with time makes the computation of its intensity function efficient, the linearity leads to serious issues by computing the survival loss:

$$\mathcal{L}_{\text{surv},k} = \int_{T_0}^T \lambda_k(s) ds = \alpha_k (T^2 - T_0^2) \quad (37)$$

where $\mathcal{L}_{\text{surv},k}$ is the survival loss of an event with type k from T_0 to T . Hence, for the same duration of time, it can generate survival losses with a totally different magnitude. For example, the intervals $[0, 1]$ and $[1000, 10001]$ have the same length, but $(1001^2 - 1000^2)$ is 2001 times larger than $(1^2 - 0^2)$. Therefore, for a given dataset, the survival loss would become extremely large after certain timestamps so that the Rayleigh process model hardly learns anything from the positive training samples from then on.

Table 4: Link prediction analysis: MRR (%), Hits@1/3/10 (%), and Categorical Proportions (%). For category 1 samples, we use $e^{h,sp}$ and $e^{h,op}$ for the object entity prediction task and the subject entity prediction task, respectively; for category 2 samples, we use $e^{h,sp}$ and $e^{h,o}$ for the object entity prediction task and the subject entity prediction task, respectively; for category 3 samples, we use $e^{h,s}$ and $e^{h,op}$ for the object entity prediction task and the subject entity prediction task, respectively; for category 4 samples, we use $e^{h,s}$ and $e^{h,o}$ for the object entity prediction task and the subject entity prediction task, respectively.

Datasets		ICEWS14 - filtered					GDELT15/16 - filtered				
Category	Link Prediction Type	Prop.	MRR	Hits@1	Hits@3	Hits@10	Prop.	MRR	Hits@1	Hits@3	Hits@10
1	object prediction	87.22	33.26	23.52	36.83	52.36	94.62	24.27	16.13	26.32	39.07
	subject prediction		28.51	19.30	31.31	47.28		24.28	16.27	26.37	38.65
	average		30.88	21.41	34.07	49.82		24.28	16.2	26.34	38.86
2	object prediction	6.19	28.51	18.55	31.82	48.2	2.52	22.42	14.15	23.91	38.68
	subject prediction		1.04	0.11	0.61	2.16		1.06	0.12	0.60	2.20
	average		14.78	9.33	16.21	25.18		11.74	7.13	12.26	20.44
3	object prediction	5.15	1.23	0.22	0.86	2.31	2.37	1.00	0.12	0.51	1.86
	subject prediction		26.38	16.8	29.11	45.69		22.13	13.74	24.15	38.52
	average		13.8	8.51	14.98	24.00		11.57	6.93	12.33	20.19
4	object prediction	1.38	6.9	3.07	6.74	13.36	0.47	6.53	2.74	6.35	13.24
	subject prediction		5.66	2.13	5.56	12.06		6.50	2.21	7.77	13.33
	average		6.28	2.6	6.15	12.71		6.52	2.47	7.06	13.28

Table 5: Time prediction analysis: MRR (%), cHits@1/3/10 (%) and Categorical Proportions (%). For category 1 samples, we use both $e^{h,sp}$ and $e^{h,op}$ for the time prediction task; for category 2 samples, we use both $e^{h,sp}$ and $e^{h,o}$ for the time prediction task; for category 3 samples, we use both $e^{h,s}$ and $e^{h,op}$ for the time prediction task; for category 4 samples, we use both $e^{h,s}$ and $e^{h,o}$ for the time prediction task.

Datasets	ICEWS14 - filtered					GDELT15/16 - filtered				
Category	Prop.	MAE(days)	cHits@1	cHits@3	cHits@10	Prop.	MAE(hours)	cHits@1	cHits@3	cHits@10
1	87.22	3.64	72.73	85.04	93.91	94.62	4.4	60.73	78.59	91.31
2	6.19	6.97	56.63	72.20	87.35	2.52	7.84	45.88	68.28	86.04
3	5.15	8.77	54.12	70.58	85.26	2.37	7.00	47.16	68.80	86.32
4	1.38	19.71	53.55	65.48	76.83	0.47	2.30	72.99	86.5	95.15

C Analysis of the GHN’s Performance

The relevant historical event sequence is the key for the Graph Hawkes Network to extract information for prediction tasks. Taking object prediction as an example, GHN aims to estimate the most possible object entity for the query $(e_{s_i}, e_{p_i}, ?, t_i)$ based on its relevant historical event sequence $e^{h,sp}$. However, based on the definition in Section 4.1, the relevant historical event sequence $e_i^{h,sp}$ requires that the predicate and the subject entity of each included historical event should be the same as that of the query $(e_{s_i}, e_{p_i}, ?, t_i)$, leading to the fact that a considerable amount of queries do not have this kind of relevant historical events, which significantly harm the predictive performance of the GHN. Thus, we define the second type of relevant historical event sequence that consists of the events that contain the same subject entity e_{s_i} as the query $(e_{s_i}, e_{p_i}, ?, t_i)$ but different predicate e_{p_i} . We denote this type of relevant historical event sequence as $e_i^{h,s}$ with the following definition:

$$e_i^{h,s} = \{ \bigcup_{0 \leq t_j < t_i} (e_{s_i}, \mathbf{O}_{t_j}(e_{s_i}), t_j) \}. \quad (38)$$

Similarly, we define a relevant historical event sequence $e_i^{h,o}$ that contains the same object entity e_{o_i} as the subject prediction query $(?, e_{p_i}, e_{o_i}, t_i)$ but a different predicate e_{p_i} as follows:

$$e_i^{h,o} = \{ \bigcup_{0 \leq t_j < t_i} (e_{o_i}, \mathbf{S}_{t_j}(e_{o_i}), t_j) \}. \quad (39)$$

To analyze the predictive performance of the GHN, we classify the test set into four categories: category 1 samples have both $e^{h,sp}$ and $e^{h,op}$; category 2 samples only have $e^{h,sp}$; category 3 samples only have $e^{h,op}$; category 4 samples have neither $e^{h,sp}$ nor $e^{h,op}$. As mentioned in Section 4.1, to handle samples without $e^{h,sp}$ or $e^{h,op}$, we use $e^{h,s}$ and $e^{h,o}$ for prediction tasks, respectively. Taking samples belonging to the category 2 as an example, for a query $(e_{s_i}, e_{p_i}, ?, t_i)$, we use $e_i^{h,sp}$ to predict its object entity; for a query $(?, e_{p_i}, e_{o_i}, t_i)$, we use $e_i^{h,o}$ to predict its subject entity; for a query $(e_{s_i}, e_{p_i}, e_{o_i}, ?)$, we use both $e_i^{h,sp}$ and $e_i^{h,o}$ to predict its time.

The performance of the link prediction and the time prediction for each category is shown in Table 4 and 5 that clearly demonstrates the superiority of the GHN for data samples that have historical event sequences. Taking the link prediction as an example, the GHN achieves a good performance for both subject prediction and object prediction when the data sample $(e_{s_i}, e_{p_i}, e_{o_i}, t_i)$ belongs to the first category because those data samples have both $e^{h,sp}$ and $e^{h,op}$, which can be utilized for prediction. Besides, the GHN performs well for object prediction when the test quadruple $(e_{s_i}, e_{p_i}, e_{o_i}, t_i)$ belongs to the second category; however, the GHN has poor performance for subject prediction given a query $(?, e_{p_i}, e_{o_i}, t_i)$ because those data samples do not have $e^{h,op}$, in other words, the object e_{o_i} had not been linked with any subject entities under the predicate e_{p_i} in the past. Therefore, it is hard to predicate the subject e_{s_i} for the given query. Similarly, the GHN only performs well for subject prediction when the test quadruple $(e_{s_i}, e_{p_i}, e_{o_i}, t_i)$ belongs to the third category. Moreover, the GHN achieves the poorest predictive performance only when test quadruples belong to the fourth category, which have neither $e^{h,sp}$ nor $e^{h,op}$. Thus, the GHN outperforms all other state-of-the-art models as long as the given query has relevant historical events.